Available online at www.sciencedirect.com
SCIENCE DIRECT
Journal of Catalysis 242 (2006) 162–171
JOURNAL OF CATALYSIS
www.elsevier.com/locate/jcat

Selective hydrogenation of crotonaldehyde on Au/HSA-CeO_2 catalysts

Betiana Campo [a], María Volpe [a,*], Svetlana Ivanova [b], Raymonde Touroude [b]

[a] *PLAPIQUI, camino Carrindanga km 7, 8000 Bahia Blanca, Argentina*
[b] *LMSPC, UMR 7515 du CNRS, ECPM, ULP, 25, rue Becquerel, 67087 Strasbourg Cedex 2, France*

Received 22 February 2006; revised 19 May 2006; accepted 22 May 2006
Available online 7 July 2006

Abstract

The gas-phase hydrogenation of crotonaldehyde was carried out over Au supported on high-surface area (HSA) CeO_2, previously reduced at 120 °C. The products analyzed during the initial, nonequilibrium stage showed the formation of large amounts of ethanol, which rapidly decreased with time on stream and were replaced by a combination of condensation products (mainly 2,4,6-octatrienal) under equilibrium conditions. The production of crotyl alcohol largely exceeded that of butanal at any time on stream. Under steady-state conditions, the crotyl alcohol-to-butanal ratio was equal to 1.7. When the catalyst was recalcined in air at 300 °C, just before the reduction treatment, the formation of ethanol in the initial stage and that of condensation products under steady state decreased. Besides, notable increase in the production of crotyl alcohol was observed, whereas butanal formation was unaffected. Finally, Au/HSA-CeO_2 is a highly selective catalyst for C=O bond hydrogenation when crotyl alcohol/butanal ratio is equal to 3 under a steady-state regime. These results were compared to those obtained for Au/TiO_2 [R. Zanella, C. Louis, S. Gorgio, R. Touroude, J. Catal. 223 (2004) 328]. The role of acid–base sites, as well as that of the redox centers of HSA-CeO_2, is evaluated. Even though ceria sites are engaged in the reaction, the catalytic properties of Au/HSA-CeO_2 are attributed mainly to the gold nanoparticles.

Keywords: Au/CeO_2; Ceria; Selective hydrogenation; Gold catalysts; Crotonaldehyde hydrogenation

1. Introduction

It has been demonstrated that heterogeneous gold catalysts, when prepared in an appropriate manner, are active and selective for a number of reactions. The key point is preparation of the supported gold catalysts, where the metal particles should be within the nanometer size range [1]. The most remarkable results for gold nanoparticles have been found in oxidation reactions, such as CO and VOC oxidation [2,3]. However, for hydrogenation reactions, gold has always been considered poorly reactive because of its low ability to dissociate H_2 [4].

Even if gold catalysts are not as active, they are more promising than conventional metal hydrogenation catalysts because of their higher selectivity, in, for instance, the selective hydrogenation of α,β-unsaturated aldehydes and ketones, where the challenge lies in hydrogenating the C=O bond preferentially over the C=C bond [5]. Conventional monometallic hydrogenation catalysts (Ni, Pd, and Pt), deposited on silica or alumina supports, produce saturated aldehyde as the main product [6–8]. However, using reducible oxide as a support has a significant beneficial effect on selectivity. For Pt supported on TiO_2 [9,10], ZnO [11], SnO_2 [12], or CeO_2 [13,14], 50–90% crotyl alcohol selectivity was observed (in the steady state) for crotonaldehyde hydrogenation.

Regarding the triad of group I metals, copper should be considered intrinsically unselective for the hydrogenation of α,β-unsaturated compounds [15]. Treatment with thiophene is necessary to improve the catalytic performance [16]. On the other hand, silver [17–21] and gold [22–31] catalysts lead to relatively high selectivity to the desired product, with no sophisticated catalyst preparation required, demonstrating that a particular property of gold and silver nanoparticles is their intrinsic selectivity toward hydrogenation of the conjugated C=O bond. In addition, the nature of the support has some influence on activity and selectivity.

* Corresponding author.
E-mail address: mvolpe@plapiqui.edu.ar (M. Volpe).

0021-9517/$ – see front matter
doi:10.1016/j.jcat.2006.05.031

Focusing our attention on selective gold catalysts for the hydrogenation of α,β-unsaturated compounds, we find various explanations of how the support affects the catalytic behavior of gold. Milone et al. [26,27] concluded that the selectivity toward unsaturated alcohol is strongly influenced by the support and increases with its reducibility; they suggested that an electron transfer creates electron-enriched gold particles on which the C=O bond is activated. Regarding crotonaldehyde hydrogenation, Bailie and Hutchings [23] showed that Au/ZrO_2 and Au/ZnO are quite selective. They demonstrated that selectivity can be enhanced by pretreatment with thiophene and suggested that sites at the Au–support interface could be responsible for the carbonyl activation. The effect of thiophene was to modify these interface sites or to create new sites on the support. An increase in up to a value of 80% was found on Au/ZnO when the catalyst was reduced at high temperature (400 °C) [24]. It was proposed that this exceptionally high selectivity was due to the presence of large gold particles (up to 20 nm) on ZnO. For the same reaction, Okumura et al. [25] found selectivities to crotyl alcohol of 25% for Au/TiO_2 and 10% for Au/Al_2O_3 and Au/SiO_2, with the gold particle sizes for these different catalysts in a similar range (3–5 nm). The reaction would be slightly sensitive to the selection of the support for the product selectivity. On a Au/SiO_2 catalyst with similar particle sizes as those studied by Okumura et al., but using higher pressure and temperature, Schimpf et al. investigated the selective hydrogenation of acrolein over Au/SiO_2, Au/TiO_2, Au/ZrO_2, Au/ZnO, and Au-In/ZnO [29]. They found selectivities between 23 and 63% and concluded that the edges of single crystallites are the active sites for the preferred C=O hydrogenation. The support intervenes only to determine the morphology of the particles.

For Au/TiO_2, Zannella et al. [30] studied the affects of the preparation method, gold particle size, and reaction temperature in the 80–160 °C range, as well as the concentration of oxygen vacancies at the gold–titania interface, on the hydrogenation of crotonaldehyde. They found that the reaction rate was sensitive to particle size, whereas the selectivity was independent of reaction temperature, preparation method, and reduction pretreatment, demonstrating that oxygen vacancies are not involved in the reaction.

The logical approach for the further investigation of this peculiar behavior of gold catalysts in the selective hydrogenation of α,β-unsaturated carbonyl compounds is to compare gold catalysts deposited on different supports. Consequently, here we report the results obtained for crotonaldehyde hydrogenation over gold supported on high-surface area ceria (Au/HSA-CeO_2). The reaction was performed under the same experimental conditions as for Au/TiO_2 [30]. To the best of our knowledge, this is first time that Au/HSA-CeO_2 has been used in the hydrogenation of crotonaldehyde. Previously, Au/CeO_2 was used mainly in the water–gas shift reaction [32] and the combustion of volatile compounds [33], where ceria plays an active role by supplying oxygen.

In this work, attention was focused on the influence of the gold–support interaction on the selectivity to different products, as well as the role of Lewis acid and basic sites and redox properties of the ceria in the reaction.

2. Experimental

2.1. Catalyst preparation

Ceria from Rhône Poulenc (Acalys HSA 5) with a surface area of 240 $m^2\,g^{-1}$ and a pore volume of 0.2 $ml\,g^{-1}$ was used as a support, and $HAuCl_4{\cdot}xH_2O$ (Alfa Aesar) was used as a gold precursor. Before preparation, CeO_2 was dried in air at 500 °C for 1 h.

The catalyst was prepared by the deposition–precipitation method with sodium bicarbonate. The support was mixed at 70 °C with aqueous solution containing the desired amount of gold. The pH of the solution was adjusted to 8 by adding dropwise 0.1 M Na_2CO_3 solution under vigorous stirring. The suspension was filtered, and the catalyst precursor was washed with ammonia solution (4 $mol\,L^{-1}$) to eliminate Cl^- and then with hot water (80 °C) to wash off the Na^+ ions. The catalyst was then dried at 100 °C for 12 h and calcined under air at 300 °C (1 °C/min) for 4 h before being stored in a sealed vessel.

2.2. Characterization

The concentrations of Au and Ce were determined by atomic absorption spectroscopy (AAS) at CNRS, Vernaison, France. X-ray diffraction (XRD) analysis of Au/HSA-CeO_2, reduced at 120, 300, and 500 °C, was done using a Siemens D 5000 polycrystalline diffractometer with Cu$K\alpha$ radiation.

X-ray photoelectron spectroscopy (XPS) measurements were carried out with a VG ESCA III spectrometer with an Mg anode source ($K\alpha = 1253.6$ eV) without a monochromator. Before analysis, two different pretreatments were performed in situ in the preparation chamber attached directly to the analysis chamber: calcination at 300 °C and calcination at the same temperature followed by reduction at 120 °C. Charging corrections were carried out using the binding energy (BE) of Ce^{4+} ($3d_{3/2}$ $4f^0$) at 916.6 eV according to [34], because this peak is very well defined. In this case, the C (1s) peaks could not be used for a BE reference, because the line shape showed a superposition of several components.

The reducibility of the catalysts was followed by temperature-programmed reduction (TPR) in a conventional flow system. Samples were previously calcined at 300 °C and then purged with Ar at the same temperature. Afterward, the catalyst was cooled in Ar, then switched to a H_2/Ar (5%) mixture. The temperature was linearly increased up to 730 °C, and hydrogen consumption was measured with a thermal conductivity detector.

2.3. Catalytic test

The reaction was performed in a glass flow reactor operating at atmospheric pressure, as described elsewhere [35]. Before running the catalytic test, samples were submitted to one of two in situ pretreatments: (a) reduction at 120 °C for 1 h in H_2 or (b) calcination at 300 °C for 1 h with 25 $cm^3\,min^{-1}$ of air, cooling to room temperature, followed by reduction for 1 h at 120 °C. Between treatment switches, the reactor was exhaustively evac-

uated and purged with Ar. In some cases the reduction temperature was increased to 300 and 500 °C.

The crotonaldehyde (Fluka puriss, 100–200 μl) was introduced in a trap set before the reactor tube and was maintained at 0 °C to achieve a constant crotonaldehyde partial pressure of 1.6 kPa. Two catharometers, inserted in the line at the input and output of the reactor, measured the reactant pressure during the experiment. When crotonaldehyde was injected, the reactor was kept closed to avoid air contamination. Approximately 20 min later, the reactor was opened, and immediately the output signal dropped to zero value. If no adsorption occurred on the catalyst, the output signal should recover to its initial level in about 30 s, or the time it takes for gas to reach the catharometer.

The reaction products, as well as the unreacted crotonaldehyde, were analyzed at 10-min intervals on-line using a gas–liquid chromatograph equipped with a flame ionization detector and a 30-m-long, 0.5461-mm-diameter DB-Wax column (J&W Scientific). The sensitivity factors were taken from Dietz tables [36] as 1 for crotonaldehyde (CAL), crotyl alcohol (UOL), butanal (BAL), and butanol (BOL); 1.4 for hydrocarbons (HC); 0.5 for ethanol (EOL); and 2.13 for condensation products (CP). The condensation products were analyzed by a Chrompack CP-Wax-58CB column connected to a FISONS mass spectrometer, and the hydrocarbons were analyzed by a gas chromatograph equipped with a flame ionization detector and a CP-SIL5CB column.

The activity and selectivity toward the different products were measured. The activity is reported in micromoles converted per gram of catalyst and per second ($\mu mol\, s^{-1}\, g^{-1}$). The selectivity was calculated as a ratio between the desired product and the sum of all products formed.

3. Results

3.1. Characterization

The gold content in Au/HSA-CeO_2 catalyst was 1.85 wt%. Less than 200 ppm of Cl was found in the catalyst, demonstrating that the ammonia treatment during catalyst preparation efficiently eliminated chloride from the gold precursor, as has been observed for Au/Al_2O_3 catalysts [37].

XRD of Au/HSA-CeO_2 revealed the characteristic lines of a ceria structure. But when the catalyst was calcined at 300 °C and reduced at 120 °C, no line corresponding to gold compound was visible, indicating that the noble metal particles are smaller than 4 nm, the particle size limit for the XRD analysis. When XRD analysis was carried out over Au/HSA-CeO_2 samples prereduced at 300 and 500 °C, a line corresponding to Au crystalline species began to come up, although for both cases the peak was extremely broad, indicating that only negligible particle sintering could occur at high reduction temperatures. Unfortunately, no transmission electron microscopy analysis could be carried out over these samples; the recorded images showed an extremely low contrast between CeO_2 and the gold particles to give a correct analysis of those images.

An XPS spectrum of Au/HSA-CeO_2 sample calcined at 300 °C and then reduced at 120 °C is shown in Fig. 1. The Au ($4f_{7/2}$, $4f_{5/2}$) lines are well defined with single species for each doublet component, characteristic of gold in metallic state with BE values of 83.0 and 86.7 eV. The XPS transition corresponding to O (1s) is reported in Fig. 2. It presents two components at 528.9 and 531.3 eV. The integral areas corresponding to both lines are quasi-identical. The first component was assigned to the lattice oxygen of ceria [38]. The second one, at higher BE, which was much broader than the first, could be the result of the superposition of several components attributed to OH groups in different environments [39,40] and/or vacancy-influenced oxide ions [41].

XPS analysis was also performed over Au/HSA-CeO_2 after a calcination pretreatment at 300 °C. The Au peaks were much less intense than in the case of prereduced samples shown in Fig. 1. The calcined sample showed significant charging (7 eV), making the peaks extremely wide, with bad definitions for all of the elements (Au, Ce, and O). The peak maxima corresponded to the values of reduced gold species. Scirè et al. [33] reported

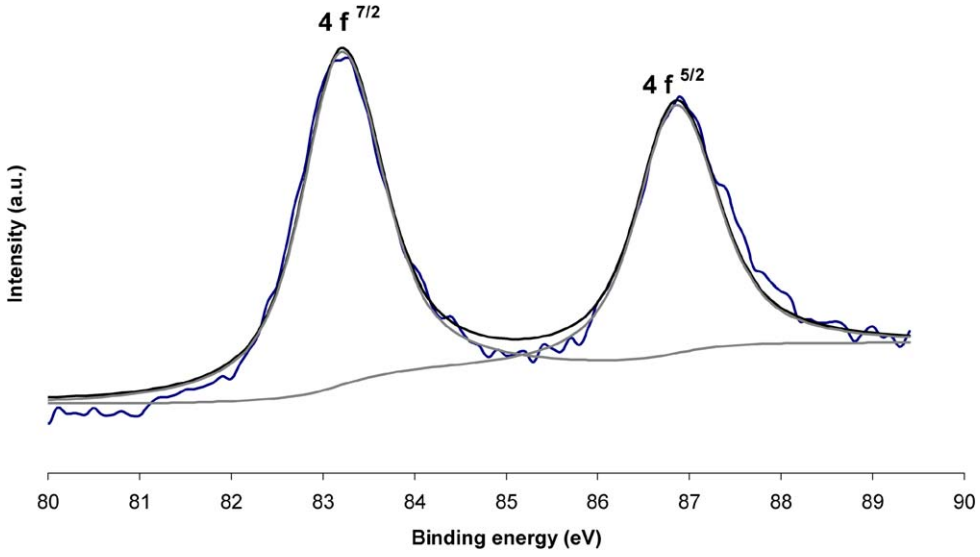

Fig. 1. XPS analysis: Au (4f) in Au/HSA-CeO_2 reduced at 120 °C.

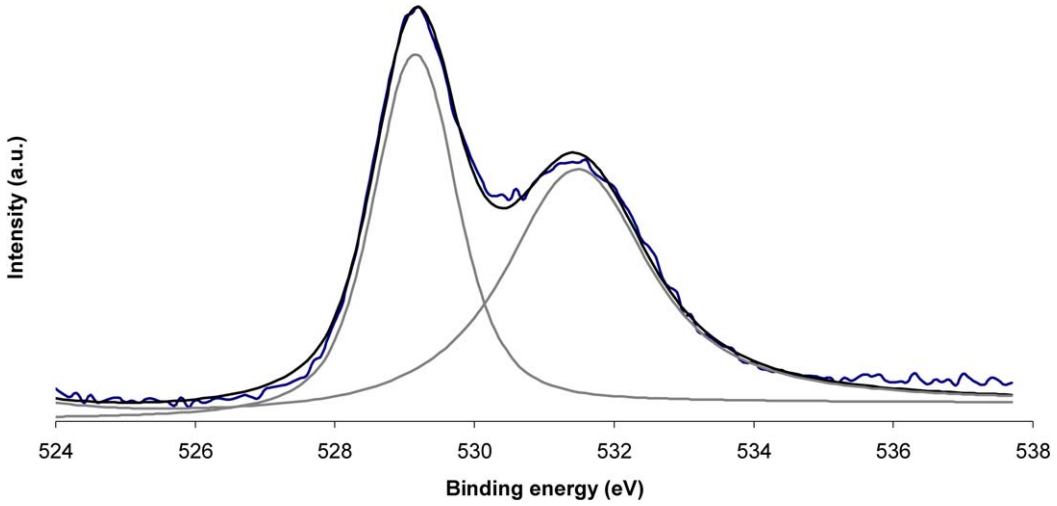

Fig. 2. XPS analysis: O (1s) in Au/HSA-CeO_2 reduced at 120 °C.

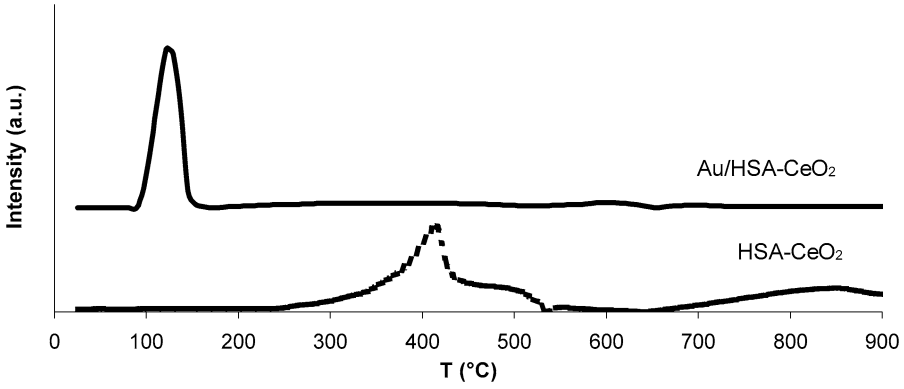

Fig. 3. TPR on HSA-CeO_2 and Au/HSA-CeO_2.

XPS spectra of Au/Ceria taken over previously calcined samples. The Au transitions were centered at values corresponding to gold in the metallic state. The quality of the Au XPS spectra is higher than in our case, probably due to the relatively high content of gold (approximately 5%) and to the lower surface area of ceria (45–105 $m^2\,g^{-1}$) compared with the ceria used in our work (240 $m^2\,g^{-1}$).

The TPR profile (Fig. 3) of the bare ceria after calcination pretreatment showed two peaks of hydrogen consumption at 430 and 850 °C. The lower reduction peak was attributed to the surface oxygen reduction (O^{2-} and O^- anions), and its contribution strongly depended on the specific surface area [42]. The higher-temperature peak was associated with the reduction of bulk oxygen and formation of lower-oxidation state cerium cations (Ce^{3+}). The presence of gold in the catalyst caused a shift of the first reduction peak to lower temperatures.

The TPR profile of Au/HSA-CeO_2 (previously calcined) shown in Fig. 3 reveals one well-defined peak with a maximum at 123 °C. This peak was associated with an H_2 consumption of 22.7 $ml\,g^{-1}$ of catalyst. Because the catalyst did not present oxidized gold species after calcination, the H_2 consumption was assigned only to the reduction of surface ceria. The quantification of the peak indicated that 30–35% of the total ceria was engaged in the redox process during the TPR experiment. Furthermore, the temperature of reduction was much lower than that corresponding to bare ceria, due to the presence of gold particles. This result was similar to that obtained by Scirè et al. [33], who reported that in 5% Au/CeO_2 prepared by a deposition–precipitation (DP) method, the reduction peak was shifted from 520 °C (pure CeO_2) to 140 °C (final catalyst). Andreeva et al. [32] found reduction peak temperatures of 110 °C for 5 wt% Au/CeO_2, 120 °C for 3 wt% Au/CeO_2, and 135 °C for 1 wt% Au/CeO_2, providing clear evidence that gold facilitates the reduction of ceria.

3.2. Catalytic results

3.2.1. Crotonaldehyde hydrogenation on Au/HSA-CeO_2: general features

Fig. 4 shows the variation of the signal of the output catharometer as a function of time on stream (TOS) for a typical catalytic run (100 mg Au/HSA-CeO_2). This variation is shown from the moment of the aldehyde injection (with a closed reactor) up to approximately 1 h TOS. After injection, the signal initially increased rapidly until it reached a constant level of H_2 and crotonaldehyde partial pressure (total pressure of 1 atm). Then the reactor was opened, and the signal, as expected, dropped to zero. It was surprising to observe that the

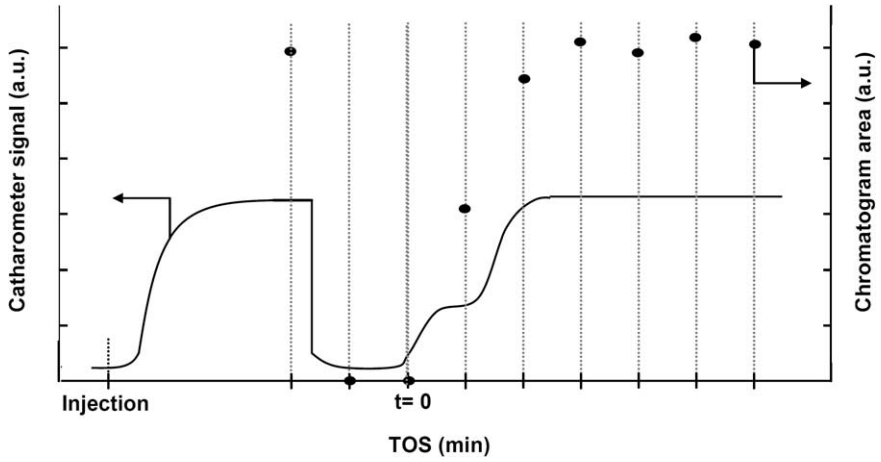

Fig. 4. Catharometer signal and chromatogram total area during a typical experiment.

Table 1
Hydrogenation of crotonaldehyde at 120 °C on Au/HSA CeO_2 reduced at 120 °C

	Nonequilibrium phase	Equilibrium phase			
		Deactivation	Quasi-steady state		
Time (min)	10	20	60	90	120
Total area	83,724	116,733	123,896	112,961	113,441
Crotonaldehyde	22,004	87,770	116,839	107,202	108,588
Hydrocarbons	142	65	0	0	0
Butanal	1079	2951	1695	1611	1395
Ethanol	26,616	728	0	0	0
Butanol	14,903	5667	151	74	92
Crotyl alcohol	18,980	18,586	3748	2841	2458
Condensation products	0	966	1463	1233	908

Note. Product chromatograph area as a function of time on stream.

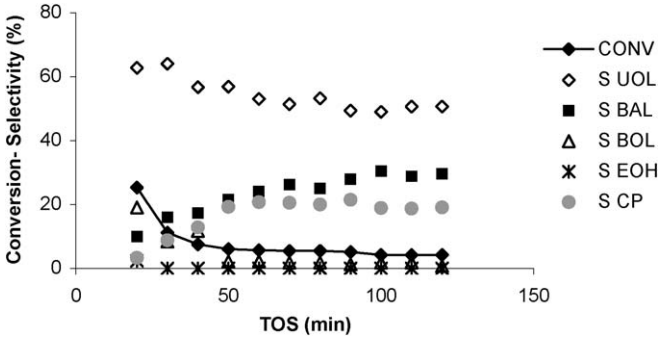

Fig. 5. Crotonaldehyde hydrogenation on Au/HSA-CeO_2 (reduced 1 h at 120 °C). Reaction temperature 120 °C.

signal did not recover its equilibrium value after the predicted short time, but did so only after approximately 20 min under a high total flow rate (30 $cm^3\,min^{-1}$), indicating that the crotonaldehyde was strongly adsorbed on the catalyst. Afterward, the signal slowly increased until it reached the input level, at which point the mass balance between the input and output products was reached. This behavior was also observed when bare CeO_2 was used. Earlier, this adsorption phenomenon was also noted over Au/TiO_2 [30] or Pt/CeO_2 [43] using the same experimental setup, but to a lesser extent, because of the lower surface area of the supports (45 and 54 $m^2\,g^{-1}$, respectively) compared with 240 $m^2\,g^{-1}$ for the ceria used here.

3.2.2. *Crotonaldehyde hydrogenation on Au/HSA-CeO_2, reduced at 120 °C (**a** pretreatment: reduction at 120 °C for 1 h in H_2)*

The reaction (total flow rate of 30 $cm^3\,min^{-1}$) was performed at 120 °C for 2 h on an Au/HSA-CeO_2 sample, initially reduced for 1 h in H_2 at 120 °C. Large variations in the product distributions were detected with TOS. A nonequilibrium reactant–solid adsorption period was observed during the first 20 min of TOS; therefore, no activity could be detected. Subsequently, equilibrium conditions were attained. Table 1 reports the chromatography area counts corrected by the molar sensitivity factors for all the products at different TOS. At 10 min TOS, mainly ethanol, butanol, and crotyl alcohol were formed, with butanal in small amounts. C_4 hydrocarbons were detected initially in trace amounts. Note that at 10 min TOS, the amount of all detected products represents 70–75% of the products detected in the equilibrium phase. The experiment was repeated to obtain the product distributions at different moments during this transient period. It should be pointed out that at initial reaction time (<10 min), ethanol was produced in relatively higher amounts.

After 20 min of TOS, the input and output mass balance was closed, and the total chromatogram area reached its maximum value. This value was maintained until the end of the experiment (Table 1). For TOS of 20–60 min, a *deactivation period* occurred, followed by a *steady-state* regime. This deactivation significantly affected the product distributions (Fig. 5). Ethanol and the hydrocarbons, detected in small amounts after 20 min TOS, disappeared quickly (Table 1). Butanol, whose formation requires two hydrogenation steps (reduction of C=O and C=C bonds), decreased rapidly to <2% at the steady state. The formation of crotyl alcohol (produced by C=O hydrogenation) was very high at 20 min TOS and then decreased to a constant level under a steady-state regime, but remained the main reaction product. Butanal (produced by C=C hydrogenation) was formed in lower amounts than crotyl alcohol at all TOSs. However, its production had a small maximum during the switch

from a nonequilibrium to a steady-state regime (Table 1). This maximum was attributed to the poisoning of the second hydrogenation step (butanal → butanol). A quite remarkable feature of this reaction was the presence of significant amounts of condensation products, which initially appeared during the equilibrium phase and reached 20% of the formed products at steady state. The main condensation product, identified by mass spectrometry, was 2,4,6-octatrienal; the other minor condensation products corresponded to different hydrogenated *cis*- and *trans*-forms of 2,4,6-octatrienal.

3.2.3. Additional reaction studies: hydrogenation of crotyl alcohol and butanal over Au/HSA-CeO_2 catalysts reduced at 120 °C

To investigate the origin of the formation and the evolution of the secondary products (hydrocarbons, condensation products, and ethanol), the hydrogenation of partially hydrogenated products (crotyl alcohol and butanal) was carried out over Au/HSA-CeO_2 reduced at 120 °C for 1 h.

With crotyl alcohol used as the reactant, the nonequilibrium period was characterized by changes in product distributions with TOS; at 10 min TOS, the main products were ethanol and hydrocarbons with selectivities of 72% and 22%, respectively. With TOS, these selectivities decreased to values below 3% and 1%, respectively, due to the increased selectivity of butanol, which reached 96% at the steady state. No condensation products were identified in this experiment, demonstrating that these products observed in crotonaldehyde hydrogenation were not formed from crotyl alcohol. In contrast, hydrocarbons and ethanol in crotonaldehyde hydrogenation also could be formed from the hydrogenation of crotyl alcohol.

However, in the hydrogenation of butanal, neither ethanol nor hydrocarbons were produced during the stabilization period. The main product was butanol (with selectivity always >95%) with minor amounts of crotyl alcohol and traces of unidentified condensation products as side products.

3.2.4. Hydrogenation of crotonaldehyde over HSA-CeO_2 prereduced at 120 °C

When crotonaldehyde was hydrogenated over CeO_2, a similar profile of the catharometer output signal was observed, revealing strong initial adsorption. At the beginning of the equilibrium phase, the conversion was approximately 8% (for Au/HSA-CeO_2 after pretreatment **a**, the conversion was 25%). The selectivity values measured for CeO_2 were 82% to crotyl alcohol, 5% to butanal, 3% to butanol, and 11% to condensation products. However, the formation of crotyl alcohol, butanal, and butanol rapidly decreased with TOS, and only condensation products were formed under the steady-state regime at a rate of 0.5×10^{-8} mol s^{-1} g $(CeO_2)^{-1}$. To make a comparison with Au/HSA-CeO_2, it is important to note that when the hydrogenation was carried out over Au/HSA-CeO_2 after pretreatment **a**, the conversion level reached at the beginning of the equilibrium phase were higher (25%) than that for bare CeO_2. For gold catalyst, a quasi-steady-state value of approximately 8% was reached, whereas the support became inactive in 20 min of TOS.

Table 2
Hydrogenation of crotonaldehyde at 120 °C on Au/HSA-CeO_2

	Red. 120 °C **a** pretreatment	Calc. 300 °C + red. 120 °C **b** pretreatment
Total area	83,724	65,433
Crotonaldehyde	22,004	1601
Hydrocarbons	142	804
Butanal	1079	0
Ethanol	26,616	2452
Butanol	14,903	50,321
Crotyl alcohol	18,980	10,255
Condensation products	0	0

Note. Product chromatograph area at 10 min on stream in nonequilibrium phase. Influence of pretreatment.

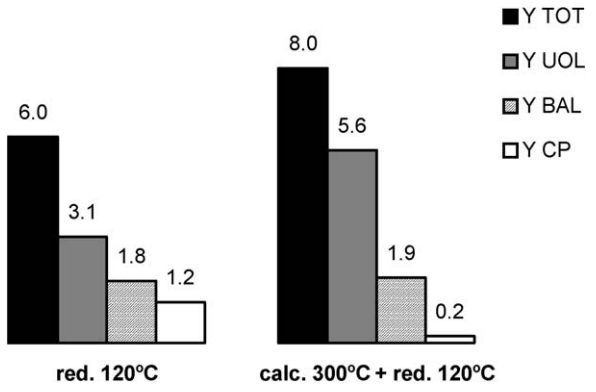

Fig. 6. Crotonaldehyde hydrogenation on Au/HSA-CeO_2 (calcined 1 h at 300 °C and reduced 1 h at 120 °C). Yields of products (10^{-8} mol s^{-1} g_{cat}^{-1}) under steady-state regime.

3.2.5. Crotonaldehyde hydrogenation over Au/HSA-CeO_2 pretreated with air before the reduction (pretreatment **b**)

In an additional experiment, the catalyst sample was calcined in situ under a flow of air at 300 °C for 1 h before reduction under a flow of H_2 for another 1 h at 120 °C. The catalytic results were compared with those obtained on the **a**-pretreated catalyst. The flow rate and the reaction temperature (120 °C) were identical for both samples.

Table 2 compares the product distributions in the nonequilibrium phase (after 10 min TOS). For pretreatment **b**, ethanol was still formed, but less so than butanol. In both cases, these two products decreased drastically with TOS to an insignificant level under steady-state conditions.

Fig. 6 compares the total activity and the yields of crotyl alcohol, butanal, and condensation products under a steady-state regime. A significant increase in crotyl alcohol and clear decrease in condensation products yield were observed on pretreatment **b** compared with pretreatment **a** case, whereas the formation of butanal was unchanged. It is worth to underline that the **b**-pretreated sample was three times more active for the hydrogenation of the C=O bond than for the hydrogenation of the C=C bond, whereas this ratio was only 1.7 for the **a**-pretreated catalyst.

Fig. 7 shows the evolution of the selectivities of various products and the conversion as a function of TOS under equilibrium conditions. As in the case with the **a**-pretreated sam-

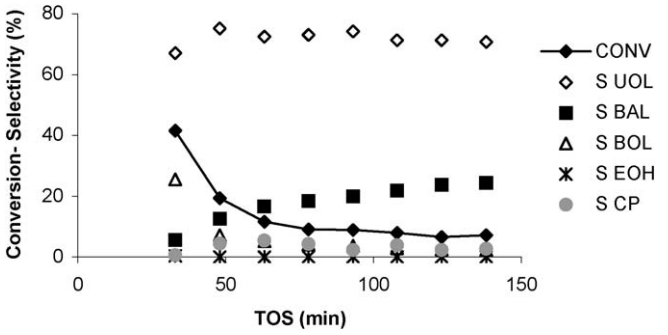

Fig. 7. Crotonaldehyde hydrogenation on Au/HSA-CeO_2 (calcined 1 h at 300 °C and reduced 1 h at 120 °C). Reaction temperature 120 °C.

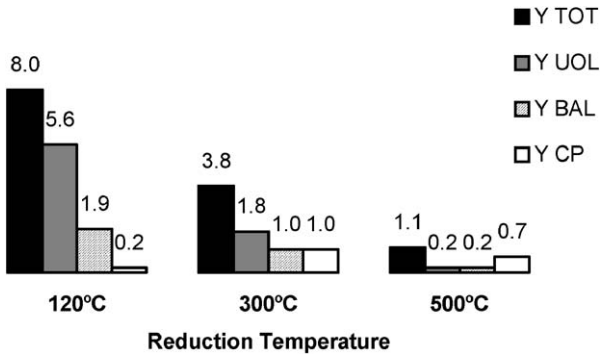

Fig. 8. Crotonaldehyde hydrogenation on Au/HSA-CeO_2 (calcined 1 h at 300 °C and reduced 1 h at 120, 300, and 500 °C). Reaction temperature 120 °C. Yield of products (10^{-8} mol s^{-1} g_{cat}^{-1}) under steady-state regime.

ple (Fig. 5), crotyl alcohol was the main reaction product at any TOS. Moreover, the selectivity to the desired product remained higher than for the **a**-pretreated samples. Therefore, the air treatment carried out before the reduction improved the catalytic behavior of Au/HSA-CeO_2. At steady state, the activity of the **b**-pretreated sample was slightly higher (33%) and the selectivity to crotyl alcohol reached 71%, compared with only 51% on the **a**-pretreated catalyst.

3.2.6. Influence of the reduction temperature of Au/HSA-CeO_2 on the crotonaldehyde hydrogenation

The following data were obtained by varying the reduction temperature to study the possibility of increasing the number of reduced sites of the ceria or to induce an interaction between the gold and the support. The treatments were performed over catalysts pretreated in air because these catalysts exhibited lower levels of condensation products and higher selectivity to crotyl alcohol.

The activities in the steady-state regime are reported in Fig. 8 as a function of the reduction temperature: 120, 300, and 500 °C. The activity decreased dramatically with increasing reduction temperature. The formation of crotyl alcohol was still predominantly affected over that of butanal. However, condensation product selectivity increased, and condensation products became the main product when the catalyst was reduced at 500 °C.

4. Discussion

The XPS and XRD characterizations of Au/HSA-CeO_2 are in agreement and indicate that after reduction at 120 °C, the catalyst constitutes small metallic gold particles (<4 nm) deposited on the ceria matrix. Moreover, TPR characterization of calcined Au/HSA-CeO_2 indicated that ceria was in a partially reduced state, suggesting that certain support sites could be engaged in the reactions of interest. The trace amount of residual chlorine in the catalysts excludes any possible effects of chloride species on catalytic performance.

The following main features became apparent from this study regarding the catalytic behavior of the Au/HSA-CeO_2 catalyst with TOS:

(i) The initial high production of ethanol, which was rapidly reduced in the process of the reaction and replaced by condensation C_8 products when gas–solid equilibrium is established.
(ii) Preferential hydrogenation of the C=O bond compared to C=C hydrogenation observed at any TOS, as well as a positive influence of in situ calcination treatment on crotyl alcohol production.

During the first 20 min of TOS, the reactions consuming large amounts of hydrogen, such as butanol and ethanol formation, were initially favored. In addition, a large amount of crotyl alcohol (product of C=O hydrogenation) was observed, whereas butanal (product of C=C hydrogenation) was formed in only minor amounts. These results prove unequivocally that the catalyst preferentially hydrogenates the C=O bond over the C=C bond.

The ethanol was a transient product, appearing in the first stage of the experiment. It was also detected when crotyl alcohol was used as substrate and not with butanal. The presence of C_4 products in the initial stage proves that ethanol (C_2H_6O) formation could result only from C=C bond scission of crotonaldehyde (C_4H_6O) or of crotyl alcohol (C_4H_8O), together with the addition of 1 oxygen and 4 or 6 hydrogen atoms, according to the stoichiometry

$$C_4H_6O \text{ (or } C_4H_8O) + 6H \text{ (or } 4H) + O \rightarrow 2C_2H_6O.$$

It is clear that the oxygen was provided by the ceria support. There are other examples in the literature in which ceria acts as an oxygen reservoir, particularly in automotive exhaust catalysts. In these cases, the catalyst works on oxidizing–reducing catalytic cycles [44]. In our experiments, pretreatment of the catalyst and the reaction occurred under hydrogen atmosphere. Therefore, the oxygen species likely came from the remaining hydroxyl groups retained on the ceria surface after the reducing pretreatment. The mechanism of formation of ethanol from crotonaldehyde could be described by

$$CH_3\text{–}CH\text{=}CH\text{–}CHO \xrightarrow{H_2,OH^-} CH_3\text{–}CHOH\text{–}CH_2\text{–}CHO \xrightarrow{H_2} 2CH_3\text{–}CH_2OH. \quad (1)$$

The first step in the ethanol formation is expected to be the hydration of the C=C bond on the ceria. In a second step, hydrogenolysis of the C(2)–C(3) bond will occur using hydrogen atoms coming from dissociated H_2 on the metallic gold particles localized in the proximity of reactive ceria sites. A similar mechanism for ethanol formation should also apply for crotyl alcohol but not for butanal, because the latter does not contain a C=C bond.

The abstraction of the ceria OH^- group by the substrate and subsequent formation of Lewis acid site on the cerium cation, as given in the following equation, could be induced by the presence of gold:

$$\text{Lewis acid site} \quad]\text{–Ce–OH} \rightarrow]\text{–Ce–}\cdot + OH^- \quad (\cdot \text{ is 2 electron vacancy}). \tag{2}$$

The noble metal weakens the Ce–O bond, as evidenced by TPR results, which showed enhanced ceria reduction (i.e., a shift of the reduction peak to lower temperature) in the presence of gold. Moreover, the hydration process of crotonaldehyde (i.e., addition of H^+ and OH^-) should be further facilitated considering gold's tendency to heterolytically dissociate H_2. This specific property of gold was proposed by Amir-Ebrahimi and Rooney [45] to explain the different catalytic behaviors of gold and platinum in the norbornadiene hydrogenation reaction. Additional experiments are needed to confirm this hypothesis in the case of crotonaldehyde hydrogenation, but because ethanol was not observed on Pt/CeO_2 [43], adopting the same explanation here is reasonable. Regardless, H_2 dissociation on gold nanoparticles or on thin gold films has been reported with no specification of the mode of dissociation (homolytic or heterolytic) [46–48].

In the second stage of crotonaldehyde hydrogenation, when equilibrium conditions were reached, ethanol disappeared, and the formation of condensation products increased. Undoubtedly, the main condensation product (2,4,6-octatrienal) was formed by aldol-condensation of two molecules of crotonaldehyde, followed by a dehydration step (Eq. (3)). In the case of an unsaturated aldehyde, which contains series of conjugated single and double bonds, the polarity of the C=O bond is delocalized along the chain due to the resonance effect. Therefore, aldol condensation occurs on the C atom in the γ-position in α,β-unsaturated aldehyde instead of on the α-C as for the saturated one. This effect is the well-known "principle of vinylogy" [49]. The aldol condensation is an acid–base catalyzed process,

$$\begin{aligned}&\text{RCHO} + H_3C^{\delta+}\text{–CH=CH–CH=O}^{\delta-}\\ &\xrightarrow{\text{base}} \text{RCHOH–CH}_2\text{–CH=CH–CHO}\\ &\xrightarrow{\text{acid}} \text{R–CH=CH–CH=CH–CHO} + H_2O\end{aligned} \quad (\text{R is CH}_3\text{–CH=CH–}). \tag{3}$$

In the case of $Au/HSA\text{-}CeO_2$ catalyst, the base sites would be oxygen vacancies created during H_2 pretreatment as given by

$$\text{Lewis base site} \quad O^{2-} \text{ (from } CeO_2) + H_2 \rightarrow V_O^0 + H_2O \quad (V_O^0 \text{ is a neutral oxygen vacancy, with 2 electrons}). \tag{4}$$

The acid site would be a Lewis center on the cerium cation created as a result of the ethanol formation as described in Eq. (2). As a consequence of catalyst pretreatment and the side reactions in the initial stages, the support is significantly modified and begins to catalyze the formation of condensation product from crotonaldehyde.

The fact that pretreatment **b** significantly diminishes the formation of ethanol in the first stage strongly suggests that air calcination pretreatment, before reduction, decreases the number of OH groups on the ceria surface and consequently decreases the number of Lewis acid sites. This was further confirmed by the decrease in condensation product formation. According to Guzman et al. [50], different dioxygen species are formed on the surface of Au/CeO_2, including adsorbed molecular O_2, superoxide and peroxide species, $O_2^{\delta-}$ $(0 < \delta < 1)$. These species react with H_2 during the reduction treatment to form water and OH-free ceria surface, as shown in the following equation for the particular case of superoxo species:

$$Ce^{4+}(O_2^-)_2 + 2H_2 \rightarrow CeO_2 + 2H_2O. \tag{5}$$

It is important to note that if ceria was calcined for a long time before the reduction treatment, then the dioxygen species could decompose, and the reduction could lead to a fully hydroxylated surface as in the case of pretreatment **a**. Therefore, dehydroxylated ceria prepared by consecutive oxidation and reduction cycles (pretreatment **b**) is a more appropriate support for the gold particles in the selective hydrogenation of crotonaldehyde, because the formation of secondary products is minimized.

Although the sites responsible for formation of ethanol were localized on the ceria in the vicinity of the gold particles, because the latter provide the hydrogen for the hydrogenolysis of the C–C bond, the formation of condensation product could occur on bare ceria surface via its acid–base sites. The rates of condensation product formation for **a**- and **b**-pretreated catalysts and the bare ceria were 1.2, 0.2, and 0.5 ($\times 10^{-8}$ mol s^{-1} g_{cat}^{-1}) for standard reaction conditions. The difference in rates indicates that the number of acid–base sites of ceria (active for the vinylogy process) depends on the presence of gold, as well as on the type (air or/and H_2) and the temperature of the pretreatment. This is another example of the versatility of the catalytic properties of ceria.

As emphasized previously, the main hydrogenated products formed under steady-state conditions are crotyl alcohol and butanal. It is worth pointing out once again the high selectivity of C=O bond hydrogenation with $Au/HSA\text{-}CeO_2$ and recalling that this was also the case for Au/TiO_2 [30] and Au/SiO_2 [M. Abid, J.P. Abid, R. Touroude, unpublished results] for the same reaction and conditions. Therefore, this clear preference appears to be an intrinsic property of the gold nanoparticles. Several works on the selective hydrogenation of α,β-unsaturated aldehydes also confirm this finding [31].

To further extend the discussion on the selective properties of $Au/HSA\text{-}CeO_2$ catalyst in crotonaldehyde hydrogenation, we compare the results described here with those obtained under the same reaction conditions on Au/TiO_2. In the latter catalyst, Zanella et al. [30] found that the activity increased

from 0.7 to 23 μmol s^{-1} g_{Au}^{-1} when gold particle size decreased from 9 to 1.5 nm following a typical curve of evolution of the number of low-coordinated sites in the cubo-octahedral metal particles. It is interesting that the activity of our Au/CeO_2 catalysts is within this range as Au/TiO_2 catalysts, 2.7 μmol s^{-1} g_{Au}^{-1} for **a**-pretreated catalyst and 4.1 μmol s^{-1} g_{Au}^{-1} for **b**-pretreated catalyst. In terms of selectivity to crotyl alcohol, in the steady state (if condensation products are not considered) it was 63% for the **a**-pretreated catalyst, which is similar to that found on Au/TiO_2 (60–70% regardless of pretreatment), and 75% for the **b**-pretreated catalyst. Continuing with the comparison between Au/TiO_2 and Au/HSA-CeO_2, the decreased activity due to an increase in reduction temperature from 120 to 500 °C was much more important in ceria than in titania-supported catalysts. The hydrogenation activity for Au/CeO_2 was divided by 10, compared with only by 2–3 on Au/TiO_2. On Au/TiO_2 the particle sizes increased from 1.7 to 2.6 nm when the reduction temperature increased from 120 to 500 °C. On Au/CeO_2, XRD analysis reveals that the sintering is quite negligible. It could hardly induce a large decrease in hydrogenation rates. An embedding of the metal particles by the reduced ceria could be suspected. Similar phenomenon like decoration of the metal particles by reduced ceria species has been often suggested in the studies on M/CeO_2 systems [51–53]. Generally this process was found to occur at reduction temperatures above 873 K. In our case, the temperature could be lower (773 K) because the surface area of the support was very large.

Examining the effect of the in situ calcination for Au/HSA-CeO_2 catalyst reveals that pretreatment **b** led to a significant increase in the production of crotyl alcohol while maintaining the same level of butanal production on **a**-pretreated catalysts. Thus, the number of sites for C=C bond hydrogenation were not affected by the oxidation–reduction cycle, but additional sites were created for the C=O bond hydrogenation. Taking into account that the acid sites involved in the formation of condensation products were largely reduced with the **b**-pretreated samples (Fig. 6), it can be proposed that the Lewis base sites (oxygen vacancies) situated at the periphery of the gold particles can be involved in the C=O hydrogenation process. The amounts of Lewis acid sites were negligible in this case, because only minor amounts of ethanol were initially produced. It has been shown [54] that oxygen vacancies (V_O^0) created in the ceria during the reduction process can exhibit redox properties according to the following equation:

$$V_O^0 + Ce^{4+} \Leftrightarrow Ce^{3+} + e^-. \quad (6)$$

When V_O^0 sites are engaged in condensation products formation, as in the case of **a**-pretreated sample, the formation of Ce^{3+} centers would not be favored. Crotyl alcohol formation is greater when the equilibrium (6) is displaced to the right. Thus, the selectivity is increased by the redox properties of the support.

5. Conclusion

Our findings indicate that Au/HSA-CeO_2 catalyst is active in the hydrogenation of crotonaldehyde at 120 °C and atmospheric pressure, with high selectivity toward the C=O carbonyl bond when pretreated in H_2 at 120 °C. This high selectivity is an intrinsic characteristic of gold nanoparticles. In addition, when calcination in air at 300 °C was carried out immediately before the reduction pretreatment, both the activity and the selectivity increased.

A detailed study of the evolution of all products formed in the reaction with TOS showed predominant initial formation of ethanol, which disappeared with TOS to be replaced by condensation products. This formation was more pronounced when the catalyst was not calcined just before the reduction. The formation of ethanol (hydration of the crotonaldehyde C=C bond followed by hydrogenolysis of the C_2–C_3 bond) requires the contribution of both the support (which provides hydroxyls) and gold to dissociate hydrogen molecules. Dehydroxylation of ceria due to ethanol formation created Lewis acid sites that were subsequently involved in the formation of condensation products together with the Lewis base sites (oxygen vacancies).

The variations in the selectivities to crotyl alcohol and butanal due to calcination pretreatment just before reduction were interpreted in terms of the intrinsic properties of gold to hydrogenate C=O and C=C bonds (C=O:C=C hydrogenation ratio = ∼2) and the additional C=O bond hydrogenation activity provided by the ceria (increasing the C=O:C=C hydrogenation ratio to 3). The redox properties of ceria gained during the oxidation–reduction pretreatment are proposed to increase the intrinsic selectivity of gold. Therefore, crotonaldehyde hydrogenation on Au/HSA-CeO_2 catalysts is governed by the intrinsic activity of gold, the nature of the ceria support, and the noble metal–support interaction. Ceria plays an important role as a result of its redox and acid–base properties. The former contributes to the enhanced selectivity to the desired product, and the latter catalyzes formation of the secondary products (ethanol in the initial stage and condensation product in the steady state).

Acknowledgments

The authors gratefully acknowledge ECOS-Sud, action No. A02E03, which allowed cooperation between two research groups from two countries. They also thank Corinne Petit and Véronique Pitchon for fruitful discussions.

References

[1] M. Haruta, T. Kobayashi, H. Sano, N. Yamada, Chem. Lett. 2 (1987) 405.
[2] C.W. Corti, R.J. Holliday, D.T. Thompson, Appl. Catal. 291 (2005) 253.
[3] G.C. Bond, D.T. Thompson, Catal. Rev. Sci. Eng. 41 (1999) 319.
[4] A.G. Sault, R.J. Madix, C.T. Campbell, Surf. Sci. 169 (1886) 347.
[5] M.A. Vannice, B. Sen, J. Catal. 115 (1989) 65.
[6] M.A. Aramendía, V. Borau, C. Jiménez, J.M. Marinas, A. Porras, F.J. Urbano, J. Catal. 172 (1997) 46.
[7] M. English, V. Ranade, J. Lercher, J. Mol. Catal. 121 (1997) 69.
[8] P. Claus, Top. Catal. 5 (1–4) (1998) 51.
[9] M.A. Vannice, Top. Catal. (1997) 241.
[10] M. Englisch, A. Jentys, J.A. Lercher, J. Catal. 166 (1997) 25.
[11] F. Ammari, J. Lamotte, R. Touroude, J. Catal. 221 (2004) 32.
[12] K. Liberkova, R. Touroude, J. Mol. Catal. A 180 (2002) 221.
[13] M. Abid, V. Paul-Boncour, R. Touroude, Appl. Catal. 297 (2006) 48.

[14] P. Concepcion, A. Corma, J. Silvestre-Albero, V. Franco, Y. Chane-Ching, J. Am. Chem. Soc. 126 (2004) 5523.
[15] G. Hutchings, F. King, I. Okoye, M. Padley, C. Rochester, J. Catal. 148 (1994) 453.
[16] G. Hutchings, F. King, I. Okoye, M. Padley, C. Rochester, J. Catal. 148 (1994) 464.
[17] J.E. Bailie, G.J. Hutchings, Catal. Commun. 2 (2001) 29.
[18] W. Grünert, A. Brückner, H. Hofmeister, P. Claus, Phys. Chem. B 108 (2004) 5709.
[19] P. Claus, P. Kraak, R. Schodel, Stud. Surf. Sci. Catal. 108 (1997) 281.
[20] P. Claus, H. Hofmeister, J. Phys. Chem. B 103 (1999) 2766.
[21] M. Bron, D. Teschner, A. Knop-Gericke, B. Steinhauer, A. Scheybal, M. Hävecker, D. Wand, R. Födisch, D. Hönicke, A. Wootsch, R. Schlögl, P. Claus, J. Catal. 234 (2005) 37.
[22] M. Shibata, N. Kawata, T. Masumuto, H. Kimura, J. Chem. Soc. Chem. Commun. (1988) 154.
[23] J.E. Bailie, G.J. Hutchings, Chem. Commun. (1999) 2151.
[24] J.E. Bailie, H.A. Abdullah, J.A. Anderson, C.H. Rochester, N.V. Richardson, N. Hodge, J.G. Zhang, A. Burrows, C.J. Kiely, G.J. Hutchings, Phys. Chem. Chem. Phys. 3 (2001) 4113.
[25] M. Okumura, T. Akita, M. Haruta, Catal. Today 2688 (2002) 1.
[26] C. Milone, R. Ingoglia, A. Pistone, G. Neri, F. Frusteri, S.J. Galvagno, J. Catal. 222 (2004) 348.
[27] C. Milone, R. Ingoglia, L. Schipilliti, C. Crisafulli, G. Neri, S. Galvagno, J. Catal. 236 (2005) 80.
[28] C. Mohr, P. Claus, Sci. Prog. 84 (4) (2001) 311.
[29] S. Schimpf, M. Lucas, C. Mohr, U. Rodemerck, A. Brückner, J. Radnik, H. Hofmeister, P. Claus, Catal. Today 72 (2002) 63.
[30] R. Zanella, C. Louis, S. Giorgio, R. Touroude, J. Catal. 223 (2004) 328.
[31] P. Claus, Appl. Catal. 291 (2005) 222.
[32] D. Andreeva, V. Idakiev, T. Tabakova, L. Ilieva, P. Falaras, A. Bourlinos, A. Travlos, Catal. Today 72 (2002) 51.
[33] S. Scirè, S. Minicò, C. Crisafulli, C. Satriano, A. Pistone, Appl. Catal. B Environ. 40 (2003) 43.
[34] A. Laachir, V. Perrichon, A. Badri, J. Lamotte, E. Catherine, J.C. Lavalley, J. El Fallah, L. Hilaire, F. Le Normand, E. Quéméré, G.N. Sauvion, O. Touret, J. Chem. Soc. Faraday Trans. 87 (10) (1991) 1601.
[35] M. Consonni, D. Jokic, D.Yu. Murzin, R. Touroude, J. Catal. 188 (1999) 165.
[36] W. Dietz, J. Gas Chromatogr. 5 (1967) 68.
[37] S. Ivanova, V. Pitchon, C. Petit, Appl. Catal. A 264 (2004) 197.
[38] J. Conesa, M. Fernandez-Garcia, A. Martinez-Arias, in: A. Trovarelli (Ed.), Catalysis by Ceria and Related Materials, in: G.J. Hutchings (Ed.), Catalysis Science Series, vol. 2, Imperial College Press, London, 2002, p. 191.
[39] B.E. Koel, G. Praline, H.I. Lee, J.M. White, R.L. Hance, J. Electron Spectrosc. Rel. Phenom. 21 (1980) 31.
[40] M. Romeo, K. Bak, J. El Fallah, F. Le Normand, L. Hilaire, Surf. Interface Anal. 20 (1993) 508.
[41] J.P. Holgado, R. Alvarez, G. Munuera, Appl. Surf. Sci. 158 (2000) 164.
[42] C. Bigey, L. Hilaire, G. Maire, J. Catal. 198 (2001) 208.
[43] M. Abid, V. Paul-Boncour, R. Touroude, Appl. Catal. 247 (2005) 48.
[44] A. Tovarelli, Catal. Rev. Sci. Eng. 38 (1996) 439.
[45] V. Amir-Ebrahimi, J.J. Rooney, J. Mol. Catal. 67 (1991) 339.
[46] E. Bus, J.T. Miller, J.A. von Bokhoven, J. Phys. Chem. A 109 (2005) 14581.
[47] M. Okada, M. Nakamura, K. Moritani, T. Kasai, Surf. Sci. 523 (2003) 218.
[48] L. Stobiński, L. Zommer, R. Duś, Appl. Surf. Sci. 141 (1999) 319.
[49] R.C. Fuson, Chem. Rev. 16 (1935) 1.
[50] J. Guzman, S. Carretttin, A. Corma, J. Am. Chem. Soc. 127 (2005) 3286.
[51] L. Kepiński, M. Wołcyrz, Appl. Catal. A 150 (1997) 197.
[52] S. Bernal, J.J. Calvino, M.A. Cauqui, J.M. Gatica, C. Larese, J.A. Perez-Omil, J.M. Pintado, Catal. Today 50 (1999) 175.
[53] S. Bernal, F.J. Botana, J.J. Calvino, G.A. Cifredo, J.A. Perez-Omil, J.M. Pintado, Catal. Today 28 (1995) 219.
[54] M. Mogensen, in: A. Trovarelli (Ed.), Catalysis by Ceria and Related Materials, in: G.J. Hutchings (Ed.), Catalysis Science Series, vol. 2, Imperial College Press, London, 2002, p. 456.